Journal for ImmunoTherapy of Cancer

T cell-intrinsic STING signaling promotes regulatory T cell induction and immunosuppression by upregulating FOXP3 transcription in cervical cancer

Huanhe Ni,[1,2] Huanling Zhang,[1] Lin Li,[1] He Huang,[3] Hui Guo,[1] Lin Zhang,[4] Chunwei Li,[1] Jing-Xiao Xu,[1,2] Cai-Ping Nie,[1,2] Kui Li,[1] Xiaoshi Zhang,[2] Xiaojun Xia ,[1] Jiang Li[1,2]

To cite: Ni H, Zhang H, Li L, *et al*. T cell-intrinsic STING signaling promotes regulatory T cell induction and immunosuppression by upregulating FOXP3 transcription in cervical cancer. *Journal for ImmunoTherapy of Cancer* 2022;**10**:e005151. doi:10.1136/jitc-2022-005151

► Additional supplemental material is published online only. To view, please visit the journal online (http://dx.doi.org/10.1136/jitc-2022-005151).

HN and HZ contributed equally.

XX and JL are joint senior authors.

Accepted 29 August 2022

For numbered affiliations see end of article.

Correspondence to
Dr Jiang Li;
lijiang2@mail.sysu.edu.cn

Dr Xiaojun Xia;
xiaxj@sysucc.org.cn

ABSTRACT

Background Stimulator of interferon genes (STING) is an innate immune sensor of cytoplasmic double-stranded DNA originating from microorganisms and host cells. The activation of cytosolic DNA-STING pathway in tumor microenvironments is usually linked to more robust adaptive immune responses to tumors, however the intracellular function of STING in regulatory T cells is largely unknown. In the present study, we aimed to explore the contribution of intracellular STING activation to regulatory T cell induction (iTreg) in cervical cancer (CC) microenvironments.

Methods Blood samples and tumor specimens were obtained from patients with CC. The intratumoral STING, CCL22, CD8 and forkhead box P3 (FOXP3) expression levels were measured by immunohistochemistry. T cell-specific STING conditional knockout mice (CD4-Cre/STING$^{flox/flox}$, TKO) were generated, and syngeneic TC-1 tumor model were investigated. The differentiation and molecular regulatory pathway of human and murine iTreg under different treatments were investigated by ex vivo assays, immunoblotting and quantitative PCR. Tumor-associated exosomes (T-EXO) were isolated from CC cell lines and exosomal contents were identified by ELISA and Western blot analysis. The impact of T-EXO on T cell differentiation was tested in in vitro cell culture.

Results Increased STING, CCL22 level, FOXP3$^+$ cells but decreased CD8$^+$ cells in tumor tissues predicted poor survival. Tumor-bearing CD4-Cre-STING$^{flox/flox}$ (TKO) mice displayed slower tumor growth tendencies as well as fewer FOXP3$^+$ cells but higher CD8$^+$ cell proportion in tumor tissues than wild-type (WT) mice. Activating of STING signaling cooperated with T cell receptor, interleukin-2 receptor and transforming growth factor-beta (TGF-β) signals to promote CD4$^+$CD25^{high}FOXP3$^+$ iTreg differentiation from both human and murine CD4$^+$-naïve T cells from WT and IFNAR$^{-/-}$ mice but not TKO or IRF3$^{-/-}$ mice in vitro. Ectopic STING, TBK1 or IRF3 expression promoted iTreg differentiation from human CD4$^+$-naïve T cells. T cell-intrinsic STING activation induced FOXP3 transcription through TBK1-IRF3-mediated SMAD3 and STAT5 phosphorylation independent of interferon-β. In CC, tumor-derived exosomes activated STING signaling in tumor-infiltrated T cells by exosomal TGF-β, cyclic GMP-AMP synthase and 2'-3'-cGAMP, leading to iTreg expansion.

Conclusions These findings highlight a novel mechanism for iTreg expansion mediated by tumor-derived exosome-activated T cell-intrinsic STING signal, and provide a rationale for developing immunotherapeutic strategies targeting STING signal in CC.

INTRODUCTION

Stimulator of interferon (IFN) genes (STING) signaling plays a critical role in host defense against viral and intracellular bacteria by regulating type I IFN signaling and innate immunity. STING has been implicated in the innate immune sensing of cancer cells, and STING signaling in immune cells is needed for type I IFN-dependent spontaneous T cell priming and natural killer (NK) cell cytotoxicity.[1–3] STING is activated via the tumor DNA-dependent activation of the cyclic GMP-AMP synthase (cGAS) and the generation of endogenous cGAMP; other cyclic nucleotides, such as cGAMP and c-di-AMP, are also exogenous STING ligands that activate type I IFN expression.[4 5] The innate immune sensing of cancer could be promoted by a cytosolic DNA-STING pathway, leading to more robust adaptive immune responses to tumors.[1] However, most of the functions of STING signaling in T cells, such as the induction of CD8$^+$ T cell apoptosis, are thought to be independent of type I IFNs.[6] Accumulating evidence suggests that elevated STING signaling is related to tumor-associated regulatory T cell (Treg) expansion[7 8]; however, the molecular mechanisms responsible for STING-mediated Treg induction are largely unknown.

Most cervical cancers (CCs) are associated with infections of high-risk human papillomavirus (HPV) strains, including HPV-16 and HPV-18.[9 10] HPV is a small double-stranded DNA (dsDNA) virus that infects squamous epithelia; in general, chronic virus infection activates STING and the type I IFN signaling pathway.[11 12] In HPV-positive cervical and oral cancers, some researchers discovered that activating STING signaling promotes tumor development by upregulating programmed cell death protein 1 (PD-1) and inducing Treg accumulation in the tumor microenvironment (TME).[13] However, the T cell-intrinsic function of STING in the progression of HPV-positive cancers is still unclear.

In the present study, we observed that high levels of intratumoral STING expression and FOXP3$^+$ cell infiltration were independent factors for unfavorable outcomes among patients with CC, and both were negatively associated with the tumor-infiltrated CD8$^+$ cell numbers. Based on this observation, we proposed that the activation of STING signaling is involved in the regulation of Treg-mediated intratumor immunosuppression. To investigate the role of STING in T cells, we employed conditional knockout mice with T cell-specific STING deficiency (CD4-Cre-STING$^{flox/flox}$, TKO) as well as IRF3 knockout (IRF3$^{-/-}$) and IFN-α/β receptor knockout (IFNAR$^{-/-}$) mice and ectopic STING expression in human CD4$^+$ T cells and further investigated the impact of STING signaling on antitumor immunity and tumor progression in CC.

MATERIALS AND METHODS

Patient information and cell culture

Fresh tumor specimens, peripheral blood (n=19) and paraffin-embedded tumor tissues (n=197) were collected from patients newly diagnosed with CC at Sun Yat-Sen University Cancer from 2008 to 2018. The detailed clinical data are described in online supplemental table S1. Peripheral blood was obtained from healthy donors.

TILs were isolated from fresh tumor specimens by mincing, digested by collagenase type IV (Sigma-Aldrich, St. Louis, Missouri, USA) and then cultured in 12-well plates in X-VIVO-15 medium (Lonza, Walkersville, Maryland, USA) for 2–3 days.

Separation of peripheral blood mononuclear cells (PBMCs) was performed by Ficoll (Thermo, Rockford, Illinois, USA) and density gradient centrifugation. The HeLa and SiHa cell lines were maintained in our laboratory in 1640 medium (Gibco, Grand Island, New York, USA) supplemented with 10% fetal bovine serum (Excell Bio, Shanghai, China). The human HEK293T and TC-1 cell lines were purchased from American Type Culture Collection, maintained in our laboratory and cultured in Dulbecco's Modified Eagle Medium or 1640 medium (Gibco) supplemented with 10% fetal bovine serum. All of the cell lines were subjected to mycoplasma testing and were found to be free of contamination.

Mouse models

IFNAR knockout mice and CD4-CRE mice were purchased from Jackson Laboratory. IRF3 knockout mice were kindly provided by Dr Liyun Shi from Nanjing University of Chinese Medicine. STING$^{flox/flox}$ mice were purchased from Nanfang Model Biotechnology Development (Shanghai, China) and crossed with CD4-CRE mice to obtain T cell-specific STING conditional knockout mice (CD4-Cre/STING$^{flox/flox}$, TKO), and littermate STING-$^{flox/flox}$ mice were used as the WT controls. Mice were bred and maintained under specific pathogen-free conditions, and all experiments were performed according to the regulations of Sun Yat-sen University.

Syngeneic TC-1 tumor model

TC-1 (1×10^6) cells were inoculated subcutaneously into TKO and WT mice with C57BL/6 background, and tumor size was measured every 2 days.

Recombinant lentivirus and T cell transfection

Human HEK293T cells were transfected with the corresponding vectors (Δ8.9: expression vectors: VSVG=3:5:2) for 48 hours to produce lentivirus. The supernatants containing lentiviral particles were collected and stored at 4°C. Using this method, we obtained recombinant lentivirus vectors, including STING-KD, STING-OE, TBK1-KD, IRF3-KD and the corresponding controls.

For the transfection of CD4$^+$ T cells, ultracentrifuged, concentrated recombinant lentivirus was titred on a 48-well plate in the presence of 10 µg/mL polybrene (Abbott Laboratories, Abbott Park, Illinois, USA) for 3 days.

Treg induction from CD4$^+$-naïve T cells in vitro

Human CD4$^+$-naïve T cells were isolated from the PBMCs of healthy donors by negative selection using human or mouse anti-CD4 beads according to the manufacturer's (Miltenyi Biotec) instructions. Human CD4$^+$-naïve T cells were plated onto 48-well or 24-well cell culture plates precoated with an anti-CD3 antibody (OKT3, 1 µg/mL) in low-dose human IL-2 (50 IU/L) medium (CM) for 3 or 5 days under the following treatment conditions: human TGF-β (5 ng/mL), human IFN-β (10 ng/mL) or CMA (62.5 µg/mL); transfection of STING-KD, STING-OE, TBK1-KD, IRF3-KD and corresponding controls and coculture with irradiated tumor cells. After 3 or 5 days, the cells were harvested, and the proportion of Tregs was measured by fluorescence-activated cell sorting (FACS) or immunoblotting.

Murine CD4$^+$-naïve T cells were isolated from or spleens and lymph nodes of WT or TKO mice and plated in anti-CD3 monoclonal antibody (mAb) (3 µg/mL)-precoated wells in mouse interleukin-2 (mIL-2, 50 IU/L) medium (CM) as a control subgroup or in CM with more mIL-2 (200 IU/L) as the higher IL-2 subgroup for 3 or 5 days under the following treatment conditions: DMXAA (1 µg/mL); mouse TGF-β (5 ng/mL), mouse IFN-β (10 ng/mL).

Immunohistochemistry, immunoblotting and flow cytometry

For immunohistochemistry (IHC), paraffin-embedded tissues from patients with CC were continuously sectioned at a thickness of 4 µm. IHC staining was performed using antihuman STING Abs (Cell Signaling Technology, Danvers, Massachusetts, USA), antihuman FOXP3 Abs (Santa Cruz Biotechnology, California, USA), antihuman CCL22 (LSBio, Seattle, Washington, USA) or antihuman CD8 Abs (Santa Cruz Biotechnology) according to the manufacturer's instructions. All IHC analyses were scanned using the machine KFBio scanner (KFBIO, KF-PRO-020, Ningbo, China). The level of STING and the number of $FOXP3^+$ and $CD8^+$ cells were scored by the identical parameter of the software HALO (V.3.2.1851.229, New Mexico USA). The mouse tumor tissues were fixed in formalin and processed for paraffin embedding. The following antibodies were used for IHC: antimouse FOXP3 (Cell Signaling Technology) and antimouse CD8 (Cell Signaling Technology). Cut-off selection was based on X-tile (V.3.6.1; Yale University, New Haven, Connecticut, USA).

For immunoblotting, cells were lysed with RIPA lysis buffer (Beyotime, Shanghai, China), and the protein samples were then separated by sodium dodecyl sulfate-polyacrylamide gel electrophoresis and electrophoretically transferred onto polyvinylidene fluoride (PVDF) membranes (Millipore, Darmstadt, Germany). The membranes were incubated with primary antibodies specific for the indicated proteins and then with chemiluminescent HRP secondary antibodies (Protein Tech, Wuhan, Hu Bei, China).

For flow cytometry, human or mouse primary mAbs against CD4, CD25 and FOXP3 conjugated to various fluorescent dyes were purchased from BioLegend (San Diego, California, USA). In this study, $CD4^+FOXP3^+$ cells (in human freshly isolated TILs) or $CD4^+CD25^{high}FOXP3^+$ cells (induced from $CD4^+$-naïve T cells in vitro) were defined as Tregs. For Treg staining, the cells were stained for surface markers, including CD4 and CD25, and then treated with the FOXP3/Transcription Factor Staining Buffer Set (Invitrogen, Carlsbad, California, USA) for FOXP3 staining. All FACS staining was performed with fixable viability stain (BD Biosciences, San Jose, California, USA) to distinguish the live and dead cells, and all analyses were gated on the live cell population. Positively stained cells were detected using a Beckman Coulter CytExpert Flow Cytometer and analyzed using FlowJo V.10 software.

The antibodies used in this study are listed in online supplemental table S4

Quantitative RT-PCR analysis

Total mRNA was extracted from the different cells with TRIzol (Invitrogen) according to the manufacturer's protocol. Then, the mRNA was reverse-transcribed into complementary DNA (cDNA) by a RevertAid First-Strand cDNA Synthesis Kit (Thermo Scientific). Real-time PCR was performed by using ChamQ SYBR qPCR Master Mix (Vazyme). The primers used in this study are listed in online supplemental table S5.

For quantitative RT-PCR analysis, the 2xRealStar SYBR Mixture (Vazyme, Nanjing, China) was used according to the manufacturer's instructions. The mRNA levels of the indicated genes were determined using the ΔΔCt method. The data indicate the relative mRNA levels (fold induction), with the relative quantity of the control cells set to one.

Plasmids and reagents

STING-OE (#EX-NEG-Lv103) and control (OENC, #EX-E1218-Lv103) vectors were purchased from GeneCopoeia (Guangzhou, China). STING-KD, TBK1-KD and IRF3-KD were constructed from the backbone pLKO. The shRNA sequences are provided in the online supplemental table S6.

T-EXO isolation and treatment

Exosomes were isolated from the sera of healthy controls or tumor cells by ultracentrifugation. The detailed protocol was described in our previous study.[14] For some experiments, the exosomes were treated with proteinase K (100 µg/mL) for 1 hour and then heated at 95°C for 5 min before use.

ELISA detection for exosomal 2'-3'-cGAMP

The level of exosomal 2'-3'-cGAMP were measured using 2'-3'-cGAMP ELISA kits (Cayman Chemical, 501700, Michigan, USA) according to the manufacturer's instructions.

Statistical analysis

The in vitro experiments were performed a minimum of three times. The numerical data are presented as the mean±SEM. Two-tailed Student's t-test was used to compare the numerical data with GraphPad Prism V.7 (La Jolla, California, USA) or SPSS V.18.0 software (Chicago, Illinois, USA). Pearson's χ^2 test was used to analyze the correlations between immunohistochemical markers and patients' clinicopathological characteristics. Spearman's correlation was used to evaluate the relationships between two variants. Kaplan-Meier and log-rank tests were used for patient survival analyses, and univariate and multivariate Cox regression analyses were used for the proportional hazards model. All cut-off values were obtained using X-tile (V.3.6.1). The softwares used in this study are listed in online supplemental table S7. *P* values <0.05 were considered statistically significant. The abbreviations related in this study are listed in online supplemental table S8.

RESULTS

Intratumoral STING expression and the $FOXP3^+$ cell density are independent predictors in patients with CC

In the present study, we examined STING, CCL22, forkhead box P3 (FOXP3) and CD8 expression in CC cancer tissues by immunochemical staining. We observed an abundance of STING, CCL22 and $FOXP3^+$ cells in tumor tissues compared with tumor-adjacent tissues from patients with HPV-positive CC ($p<0.05$, figure 1A,B). Moreover, high STING expression, $FOXP3^+$ cell density,

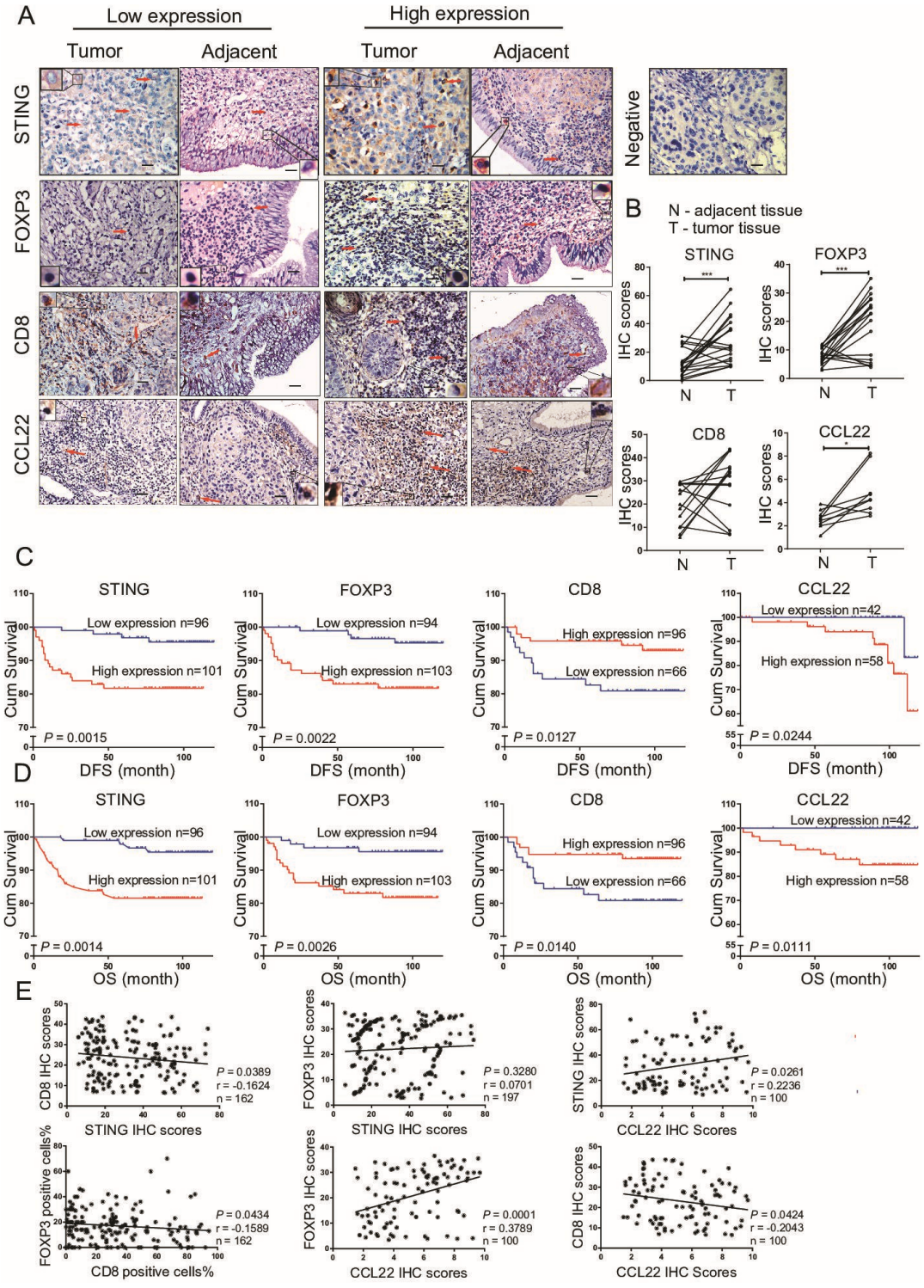

Figure 1 Intratumor STING expression, FoOXP3$^+$ cells and CD8$^+$ cells were predictors in patients with CC. (A) Representative IHC images of STING, FOXP3, CD8, CCL22 and IgG negative control in CC tumor and tumor-adjacent tissues from patients with CC. Scale bar: 50 µm. (B) The statistical graphs show the comparison of the levels of STING expression (n=19), FOXP3$^+$ cells (n=18), CD8$^+$ cells (n=14) and CCL22 (n=19) in tumor tissues and tumor-adjacent tissues from the same patient with CC. Statistical analyses were performed with a paired Student's t-test. (C–D) The Kaplan-Meier survival curves of DFS and OS rates revealed associations between the STING expression level (n=197), the CCL22 expression level (n=100) and the density of FOXP3$^+$ cells (n=197) or CD8$^+$ cells (n=162) with the prognosis of patients with CC. The cut-off value was based on X-tile analysis. (E) The correlations between STING levels and tumor-infiltrated CD8$^+$ cells, STING levels and FOXP3$^+$ cells, STING levels and CCL22 levels, FOXP3$^+$ cells and tumor-infiltrated CD8$^+$ cells, FOXP3$^+$ cells and CCL22 levels, tumor-infiltrated CD8$^+$ cells and CCL22 levels were evaluated by Spearman's correlation analysis and linear regression. R, Spearman's correlation, is the correlation coefficient. *P<0.05, ***p<0.001. CC, cervical cancer; DFS, disease-free survival; FOXP3, forkhead box P3; IHC, immunohistochemistry; OS, overall survival; STING, stimulator of interferon genes.

high CCL22 expression and low $CD8^+$ cell density in tumor tissues were significantly associated with poor disease-free survival (DFS) and overall survival (OS) in patients with CC (figure 1C,D and online supplemental table S1). We found a negative association between the intratumoral STING levels and tumor-infiltrated $CD8^+$ cell numbers and a similar association between tumor-infiltrated $CD8^+$ cells and $FOXP3^+$ cells, as well as a positive association between the intratumoral STING and CCL22 expression levels ($p<0.05$, figure 1E). The abundance of STING and reduced number of tumor-infiltrated $CD8^+$ cells were linked to advanced disease ($p<0.05$, online supplemental table S2). Multivariate analysis revealed that STING and $FOXP3^+$ cells were independent predictors in CC (online supplemental table S3).

T cell-specific STING-deficient (TKO) mice display a slow tumor growth tendency

To further explore the role of STING signaling in T cell differentiation and function, we generated a conditional knockout mouse model with T cell-specific STING deficiency (CD4-Cre/$STING^{flox/flox}$, TKO) and used littermate $STING^{flox/flox}$ mice as the wild-type (WT) controls. In TKO mice, STING expression was depleted in both $CD4^+$ and $CD8^+$ T cells compared with that in the cells of WT mice (online supplemental figure 1A,B). Accordingly, the genes downstream of STING signaling, such as IFN-β, ISG15 and IFIT1, in TKO mice were not induced by the STING agonists 2'-3'-cGAMP (cGAMP) or 5,6-dimethylxanthenone-4-acetic acid (DMXAA) (online supplemental figure 1C,D). Analysis of the T cell percentages revealed that both the $CD4^+$ and $CD8^+$ T cell percentages in TKO mice were comparable to those in WT mice in the thymus, spleen and lymphoid node (LN) tissues (online supplemental figure 1E,F), and the percentages of peripheral Tregs ($CD4^+CD25^{high}$ $FOXP3^+$ cells) were also comparable (figure 2A–C). However, on the inoculation of TC-1 (HPV^+) tumor cells into the syngeneic C57BL/6 mice, the TKO mice displayed a noticeably slower tumor growth tendency than the WT mice (figure 2D). In the tumor specimens from TKO mice, the number of tumor-infiltrated $FOXP3^+$ cells was remarkably reduced, and that of the tumor-infiltrated $CD8^+$ cells was increased compared with that in the WT mice (figure 2E,F). We also found that IFNγ expression on intratumor $CD8^+$ cells from TKO mice was increased compared with WT mice, but PD1 expression did not have significant difference (figure 2G,H). These data suggest that STING signaling in $CD4^+$ T cells is linked to tumor-derived Treg expansion and Treg-mediated tumor tolerance.

$CD4^+CD25^{high}FOXP3^+$ regulatory T cell induction generation from $CD4^+$-naïve T cells is associated with STING signaling activation

Treg expansion in the TME is associated with the generation of regulatory T cells induction (iTregs) and the recruitment of naturally occurring Tregs (nTregs).[15] To investigate the role of STING signaling in iTreg generation, we isolated $CD4^+$ T cells from the spleens of TKO and WT mice and induced $CD4^+CD25^{high}FOXP3^+$ Tregs from naïve T cells under stimulation with anti-CD3 and interleukin (IL)-2 (conditioned medium (CM)) with or without transforming growth factor-beta (TGF-β) treatment. We found that the induction efficiency of $CD4^+CD25^{high}FOXP3^+$ Tregs from $CD4^+$-naïve T cells isolated from TKO mice was much lower than that of WT mice, accompanied by a stronger activation of STING signaling (higher levels of p-TBK1 and p-IRF3) in WT $CD4^+$-naïve T cells cultured in CM or medium containing a high dose of IL-2 for 3 days (figure 3A,B). For human T cells, the short hairpin RNA (shRNA)-mediated knockdown of STING (STING-KD) in $CD4^+$ T cells reduced the $CD4^+CD25^{high}FOXP3^+$ Treg induction from $CD4^+$-naïve T cells. In contrast, forced STING overexpression (STING-OE) increased $CD4^+CD25^{high}FOXP3^+$ Treg induction from $CD4^+$-naïve T cells under CM conditions in vitro and these iTreg exhibited a high level of TGF-β, IL-10 and cytotoxic T-lymphocyte-associated protein 4 (CTLA-4) as well as a suppressive function; STING signaling was activated in $CD4^+$ T cells and STING-OE T cells but not in STING-KD T cells under CM conditions (figure 3C and D and online supplemental figure 2A-E). Furthermore, in an in vitro coculture condition mimicking the TME, HeLa and SiHa cells promoted the induction of $CD4^+CD25^{high}FOXP3^+$ Tregs and the expression of STING, p-TBK1, p-IRF3 and FOXP3 when cocultured with $CD4^+$ T cells (online supplemental figure 3A,B). The Treg induction efficiency from human $CD4^+$-naïve T cells was increased by the STING agonists cGAMP and 10-carboxymethyl-9-acridanone (CMA), accompanied by increased levels of STING, p-TBK1, p-IRF3 and FOXP3 (online supplemental figure 3C,D). Together, our data suggest that STING expression and activation are required for iTreg induction from both murine and human $CD4^+$-naïve T cells.

STING-mediated iTreg generation is independent of the type I IFN pathway

STING activation can recruit TBK1 and IRF3 to induce the production of type I IFNs.[16] In the present study, we aimed to investigate whether the type I IFN pathway is implicated in STING signaling-mediated Treg induction. The STING agonist DMXAA induced FOXP3 and p-TBK1 expression as well as iTreg generation in $CD4^+$ T cells isolated from WT and $IFNAR^{-/-}$ mice but not in those isolated from TKO mice (figure 4A,B). In addition, exogenous IFN-β did not promote iTreg differentiation from $CD4^+$-naïve T cells isolated from WT or TKO mice, but TGF-β did (figure 4C). However, the induction of Tregs was reduced in $CD4^+$-naïve T cells isolated from $IRF3^{-/-}$ mice compared with that in WT mice even in the presence of TGF-β (figure 4D). In humans, IFN-β treatment did not modulate Tregs from $CD4^+$-naïve T cells or FOXP3

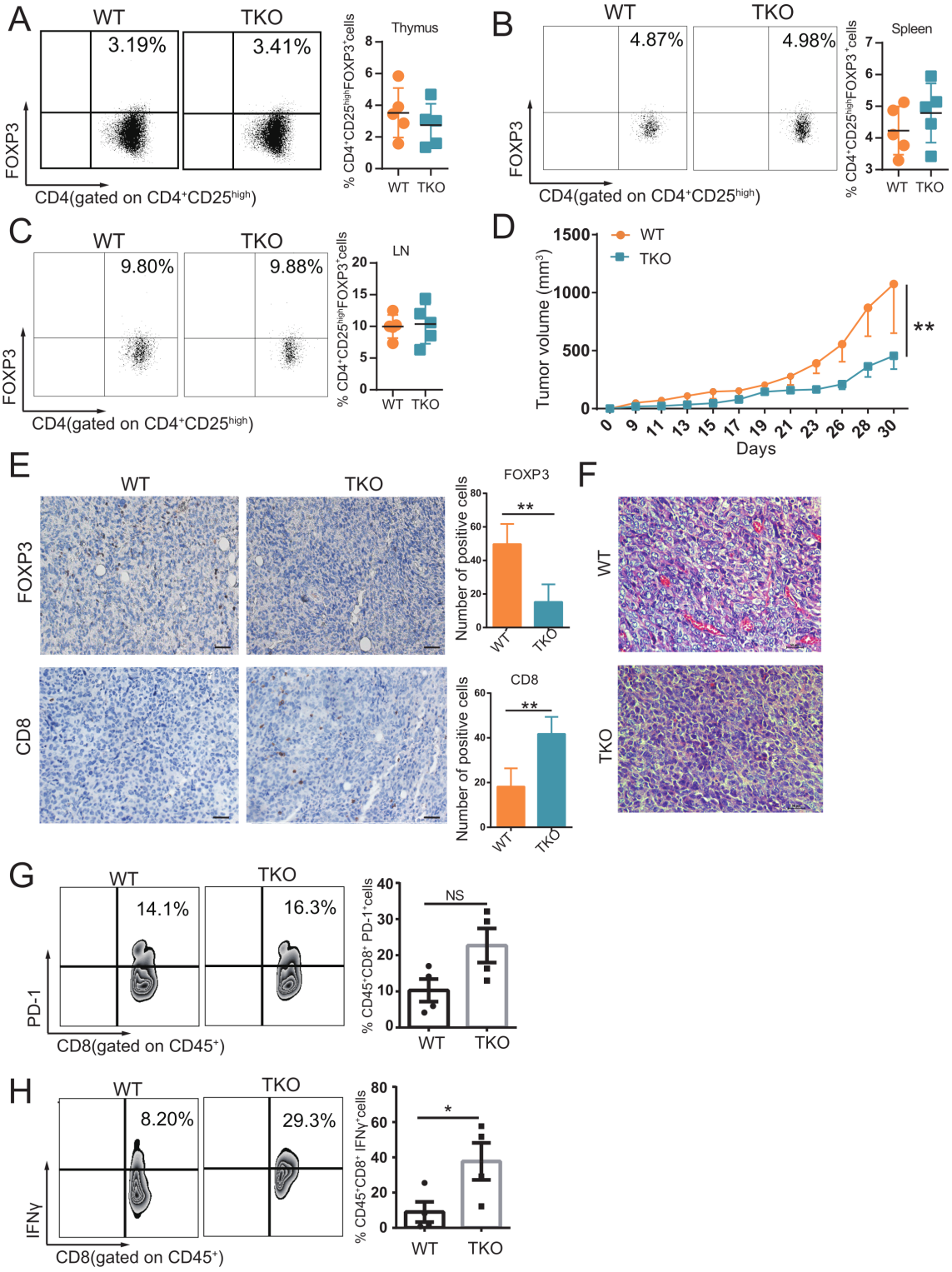

Figure 2 CD4-Cre/STING$^{flox/flox}$ (TKO) mice display a slower tumor growth tendency. (A–C) Representative images and statistical graph showing the frequencies of CD4$^+$CD25^{high} FOXP3$^+$ T cells isolated from the thymus, spleen and LN tissues of CD4-Cre/STING$^{flox/flox}$ (TKO) mice and the littermate control (WT) mice as determined by flow cytometry. (D) TC-1 cells were subcutaneously injected into WT and TKO mice, and the tumor volumes were then measured on the indicated days (n=5 per group). (E) Representative images and statistical graph showing the numbers of FOXP3$^+$ and CD8$^+$ cells in the tumor specimens isolated from TKO and WT mice as determined by IHC analysis. Quantification of the FOXP3 and CD8 area indices at high magnification (400×; *p<0.001, Student's t-test). Scale bar: 50 µm. (F) H&E staining images of TKO and WT mouse tumors. (G)–(H) Representative images and statistical graph showing the frequencies of CD45$^+$ CD8$^+$ PD-1$^+$ T cells or CD45$^+$ CD8$^+$ IFNγ$^+$ T cells isolated from TKO and WT mouse tumors. The results are representative of at least three independent experiments. All values are shown as the mean±SEM. *P<0.05, **P<0.01, Student's t-test. FOXP3, forkhead box P3; IFN, interferon; IHC, immunohistochemistry; LN, lymphoid node; NS, not significant; PD-1, programmed cell death protein 1; WT, wild-type.

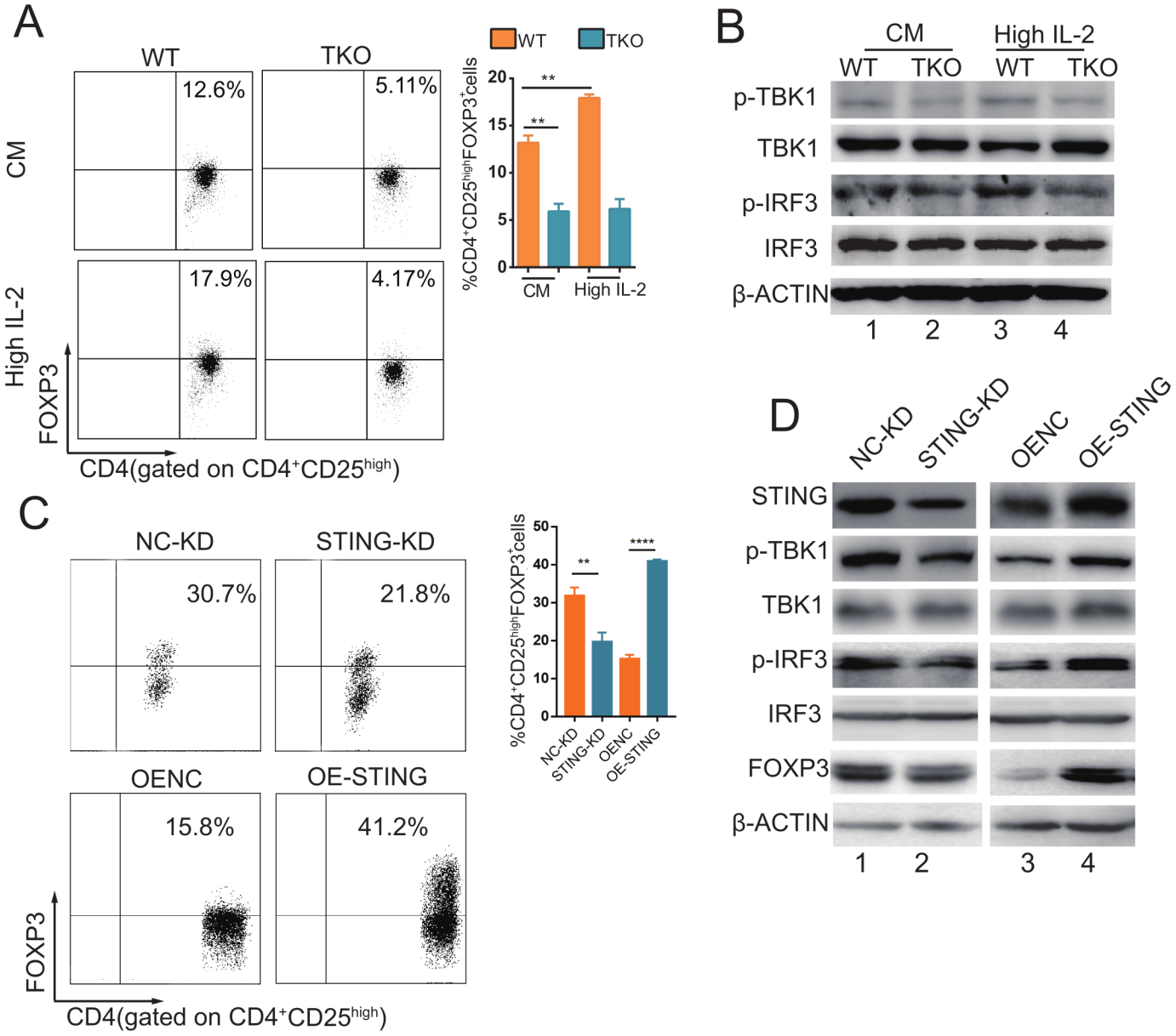

Figure 3 STING is involved in murine-induced and human-induced Treg differentiation in vitro. Murine CD4$^+$-naïve T cells were isolated from WT or TKO mice and plated in wells precoated with an anti-CD3 mAb (3 µg/mL) in mIL-2 (50 IU/L) medium (CM) as a control subgroup or in CM with more mIL-2 (200 IU/L) as the higher IL-2 subgroup for 3 days. (A) The representative FACS plot and statistical graph show the frequencies of Tregs (CD4$^+$CD25^{high} FOXP3$^+$) induced from CD4$^+$-naïve T cells isolated from WT and TKO mice under the indicated conditions. (B) Western blot analysis showed the protein expression levels of p-TBK1, TBK1, p-IRF3 and IRF3 in CD4$^+$ T cells from WT and TKO mice after culture under CM and high IL-2 conditions. β-Actin was included as a control. (C) Human CD4$^+$-naïve T cells from peripheral blood mononuclear cells were plated in wells precoated with an antihuman CD3 Ab (OKT3, 1 µg/mL) in hIL-2 (50 IU/L) medium (CM), transfected with the STING-KD vector, STING-OE vector and the corresponding lenti-control vectors (NC) and then cultured for 3 days. The FACS plot and statistical graph show the frequencies of Tregs induced from CD4$^+$-naïve T cells infected with the STING-KD, STING-OE and control vectors. (D) Western blot analysis showed the expression of STING signaling pathway proteins, including STING, p-TBK1 and p-IRF3 and FOXP3, in human CD4$^+$ T cells under the same conditions described in (C). The results are representative of at least three independent experiments. All values are shown as the mean±SEM. $^{**}P<0.01$, $^{****}P<0.0001$, Student's t-test. CM, conditioned; FACS, fluorescence-activated cell sorting; FOXP3, forkhead box P3; hIL-2, human interleukin-2; mAb, monoclonal antibody; medium; mIL-2, mouse interleukin-2; STING, stimulator of interferon genes; STING-OE, lenti-STING overexpression; STING-KD, lenti-STING knockdown; Treg, regulatory T cell; WT, wild-type.

expression (figure 4E and online supplemental figure 4A). However, knockdown of TBK1 and IRF3 decreased the induction of Tregs from human CD4$^+$-naïve T cells compared with that in the control group and reversed the promotion of iTreg differentiation mediated by STING-OE or exogenous TGF-β treatment (figure 4F-H and online supplemental figure 4B,C). Taken together, our data suggest that iTreg differentiation is largely

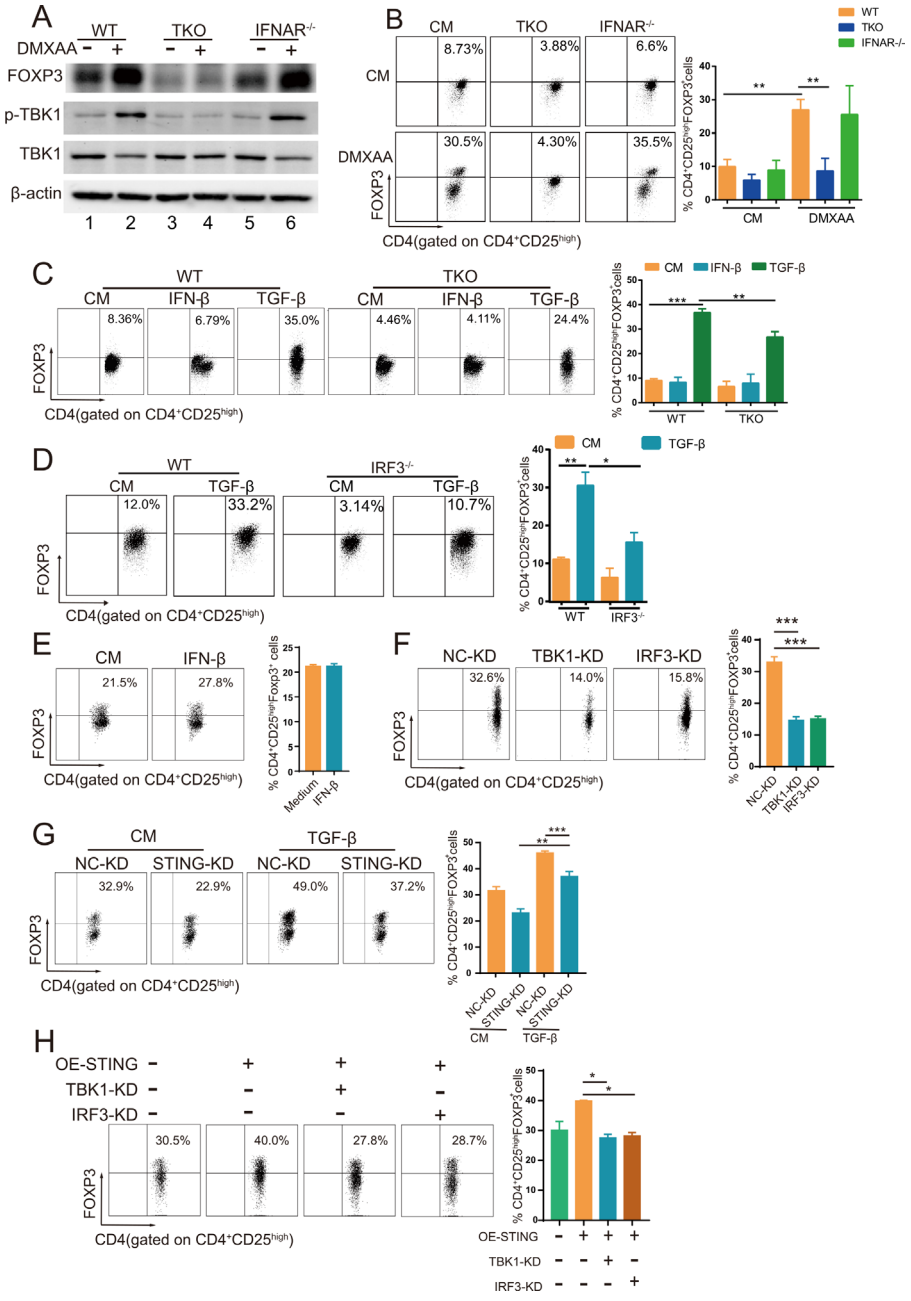

Figure 4 The STING-TBK1-IRF3 axis, not type I IFNs, mediates iTreg differentiation. Naïve CD4$^+$ T cells from WT, TKO and IFNAR$^{-/-}$ mice were treated with DMXAA (1 µg/mL) in CM for 3 days and then harvested for subsequent experiments. (A) Western blot analysis was performed with the indicated antibodies to detect FOXP3, p-TBK1 and TBK1, and β-actin was included as a control. (B) FACS plots and statistical graph showing the frequencies of CD4$^+$CD25^{high} FOXP3$^+$ Tregs induced from CD4$^+$-naïve T cells isolated from TKO, IFNAR$^{-/-}$ and WT mice. (C) Naïve CD4$^+$ T cells from WT and TKO mice were treated with IFN-β (10 ng/mL) or TGF-β (5 ng/mL) in the presence of CM for 3 days. Representative plots and statistical graphs show the proportions of Tregs induced under different treatment conditions. (D) Naïve CD4$^+$ T cells from WT and IRF3$^{-/-}$ mice were treated with mouse TGF-β (5 ng/mL) in the presence of CM for 3 days. The frequency of Tregs was assessed by flow cytometry. (E) The representative FACS plots and statistical graph show the proportions of CD4$^+$CD25^{high}FOXP3$^+$ Tregs from human CD4$^+$-naïve T cells in the presence of CM with or without human IFN-β (10 ng/mL) for 3 days. (F) The proportions of CD4$^+$CD25^{high} FOXP3$^+$ Tregs induced from human CD4$^+$-naïve T cells transfected with the TBK1-KD, lenti-IRF3-KD and corresponding control (NC-KD) vectors. (G) The proportions of CD4$^+$CD25^{high}FOXP3$^+$ Tregs induced from human CD4$^+$-naïve T cells transfected with STING-KD in CM for 3 days. (H) Forced exogenous STING expression in TBK1-KD or IRF3-KD human CD4$^+$-naïve T cells in the presence of CM. FACS plots and statistical graphs show the proportions of CD4$^+$CD25^{high}FOXP3$^+$ Tregs from human CD4$^+$-naïve T cells under different treatments. The results are representative of at least three independent experiments. All values are shown as the mean±SEM. *P<0.05, **p<0.01, ***p<0.001, Student's t-test. CM, conditioned medium; DMXAA, 5,6-dimethylxanthenone-4-acetic acid; FACS, fluorescence-activated cell sorting; FOXP3, forkhead box P3; IFN, interferon; TBK1-KD, lenti-TBK1 knockdown; STING, stimulator of interferon genes; STING-KD, lenti-STING knockdown; TGF-β, transforming growth factor-beta; Treg, regulatory T cell; WT, wild-type.

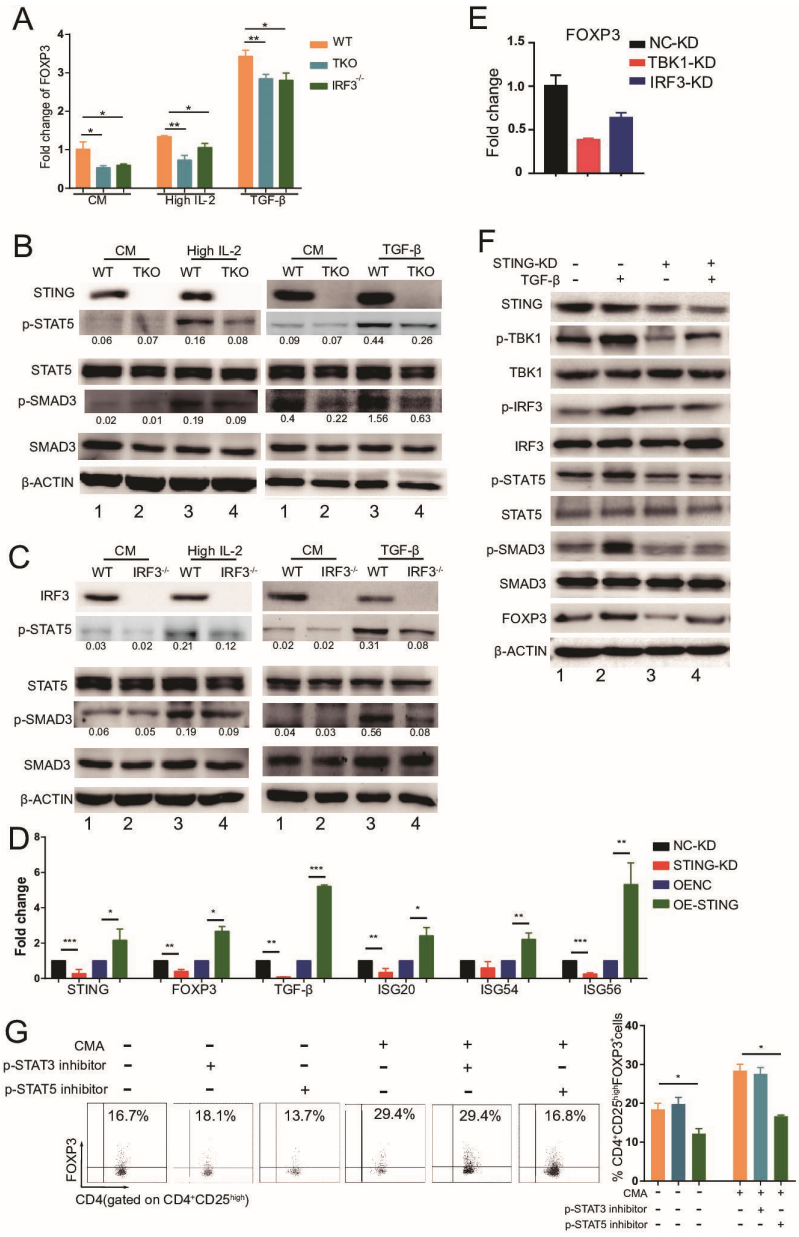

Figure 5 STING promotes FOXP3 transcription through the phosphorylation of SMAD3 and STAT5. $CD4^+$-naïve T cells from WT, TKO and $IRF3^{-/-}$ mice were cultured under the indicated conditions, including CM, high IL-2 and CM plus TGF-β (5 ng/mL) for 3 days, and then collected for qPCR analysis. (A) The statistical graph shows the fold changes in FOXP3 mRNA expression in $CD4^+$ T cells from the indicated mice under the above conditions for 3 days. (B) Western blot analysis showed the levels of the indicated proteins, including STING, p-STAT5, STAT5, p-SMAD3 and SMAD3, in $CD4^+$ T cells from WT and TKO mice after being cultured in the above conditions for 3 days. The relative intensity of the bands for p-STAT5 and p-SMAD3 was quantified by the densitormetric analysis. (C) Western blot analysis showed the levels of the indicated proteins, including STING, p-STAT5, STAT5, p-SMAD3 and SMAD3, in $CD4^+$ T cells from WT and $IRF3^{-/-}$ mice after being cultured in the above conditions for 3 days. β-Actin was included as a control. (D) The expression levels of the indicated genes, including STING, FOXP3, TGF-β, ISG20, ISG54 and ISG56, in human $CD4^+$ T cells transfected with STING-KD or STING-OE lentivirus in the presence of CM for 3 days were measured by qPCR. (E) The FOXP3 gene expression level in human $CD4^+$ T cells transfected with TBK1-KD or IRF3-KD lentivirus in the presence of CM for 3 days was measured by qPCR. (F) The indicated proteins, including STING, p-TBK1, TBK1, p-IRF3, IRF3, p-STAT5, STAT5, p-SMAD3, SMAD3 and FOXP3, in human $CD4^+$ T cells cultured in CM supplemented with TGF-β (5 ng/mL) after being transfected with the STING-KD lentivirus and the corresponding controls for 3 days were measured by western blot analysis. (G) Human $CD4^+$-naïve T cells were treated with a p-STAT3 inhibitor (cryptotanshinone, 50 ng/mL), p-STAT5 inhibitor (STAT5-IN-1, 100 ng/mL) or DMSO (as a control group) in CM for 5 days. Representative plots and statistical graphs show the proportions of Treg induced under the different treatment conditions. The results are representative of at least three independent experiments. All values are shown as the mean±SEM. *P<0.05, **p<0.01, ***p<0.001, Student's t-test. CM, conditioned medium; DMSO, dimethyl sulfoxide; FOXP3, forkhead box P3; mRNA, messenger RNA; qPCR, quantitative PCR; STING, stimulator of interferon genes; STING-KD, lenti-STING knockdown; STING-OE, lenti-STING overexpression; TBK1-KD, lenti-TBK1 knockdown; TGF-β, transforming growth factor-beta; Treg, regulatory T cell; WT, wild-type.

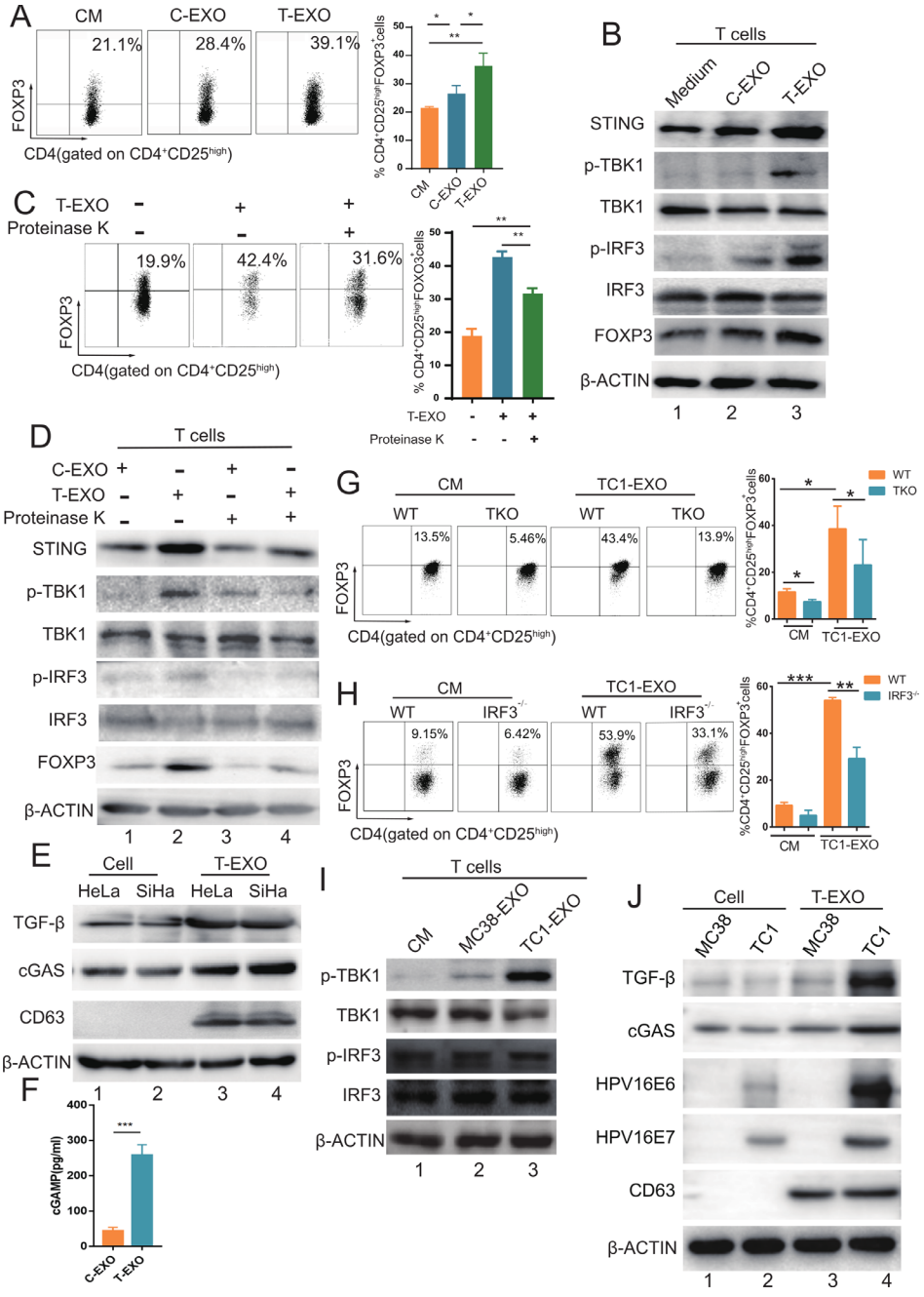

Figure 6 Tumor-derived exosomes promoted iTreg generation and STING signaling activation. Exosomes were isolated from the supernatants of HeLa cells (T-EXOs) or the plasma of healthy controls (C-EXOs). (A) The representative FACS plot and statistical graph show the proportions of Tregs from human CD4$^+$-naïve T cells in the presence of C-EXOs and T-EXOs. (B) Western blot analysis showed the levels of the indicated proteins, including STING, p-TBK1, TBK1, p-IRF3, IRF3 and FOXP3, in T cells derived from human CD4$^+$-naïve T cells in the presence of C-EXOs or T-EXOs. (C–D) T-EXOs and C-EXOs were treated with proteinase K (100 µg/mL) and then heated at 95°C for 5 min before being added to the human CD4$^+$-naïve T cell culture medium. Tregs were induced from human CD4$^+$-naïve cells in the presence of C-EXOs, T-EXOs or proteinase K-treated T-EXOs and C-EXOs. The cells were harvested for CD4, CD25 and FOXP3 FACS staining (C) or immunoblotting for the indicated proteins, including STING, p-TBK1, TBK1, p-IRF3, IRF3 and FOXP3 (D). (E) Immunoblotting showed the levels of TGF-β, cGAS and CD63 (exosome biomarker) in T-EXOs and their parental cell lines HeLa and SiHa. (F) The level of 2'-3'-cGAMP in C-EXO and T-EXO detected by ELISA. (G–H) naïve CD4$^+$ T cells isolated from WT, TKO (G) or IRF3$^{-/-}$ mice (H) were treated with TC-1-exosomes (TC-1-EXO) or not in CM for 3 days and harvested for FACS staining. Representative plots and statistical graphs show the proportion of Tregs induced under the indicative conditions. (I) Western blot analysis showed the phosphorylation of IRF3 and TBK1 when treatment with MC38 and TC-1 exsome. β-Actin was included as a control. (J) Western blot analysis showed the protein expression levels of TGF-β, cGAS, HPV16E6, HPV16E7 and CD63 in cells and exosome from the MC38 and TC-1. β-Actin was included as a control. The results are representative of at least three independent experiments. All values are shown as the mean±SEM. *P<0.05, **p<0.01, ***p<0.001, Student's t-test. FACS, fluorescence-activated cell sorting; FOXP3, forkhead box P3; iTreg, regulatory T cell induction; STING, stimulator of interferon genes; WT, wild-type.

dependent on the STING-TBK1-IRF3 pathway but independent of the type I IFN pathway.

STING activation promotes FOXP3 transcription by phosphorylating SMAD3 and STAT5

To further investigate the mechanism by which STING manipulates Treg induction in $CD4^+$ T cells, we first detected the messenger RNA (mRNA) level of FOXP3 in $CD4^+$ T cells and found that it was decreased in $CD4^+$ T cells with STING or IRF3 knockout grown in CM even in the presence of TGF-β and a high dose of IL-2 (figure 5A). Next, we examined the phosphorylation levels of SMAD3 and STAT5, which have been identified as transcriptional activators of FOXP3.[17 18] Consistent with the FOXP3 expression levels, the phosphorylation levels of SMAD3 and STAT5 were increased in $CD4^+$ T cells isolated from WT mice but not in those isolated from TKO and $IRF3^{-/-}$ mice under the above conditions (figure 5B,C, online supplemental figure 5A-D). In human T cells, the mRNA levels of FOXP3, TGF-β and the STING downstream genes ISG20, ISG54 and ISG56 were significantly altered in STING-KD, STING-OE, TBK1-KD and IRF3-KD human $CD4^+$ T cells under CM conditions (figure 5D,E). Moreover, importantly, FOXP3 transcription was also decreased in TBK1-KD and IRF3-KD T cells (figure 5F). Similar to those in the TKO mice, the expression levels of STING, p-TBK1, p-IRF3, p-STAT5 and p-SMAD3 were reduced in STING-KD human $CD4^+$ T cells grown under CM conditions with or without TGF-β (figure 5F and online supplemental figure 5E,F). Indeed, the expression levels of p-STAT5 and p-SMAD3 were markedly decreased in TBK1-KD and IRF3-KD human $CD4^+$ T cells grown under CM conditions (online supplemental figure 5G,H). Moreover, the p-STAT5 inhibitor blocked STING-mediated iTreg promotion and FOXP3 expression under treatment with the STING agonist CMA (figure 5G and online supplemental figure 5I). Our data suggest that STING activation promotes the transcription of FOXP3 by activating the phosphorylation of the FOXP3 transcriptional activators SMAD3 and STAT5, leading to the expansion of iTregs.

Tumor-derived exosomes trigger the activation of STING signaling in tumor-infiltrating lymphocytes in CC

Numerous studies have revealed that T-EXOs carrying bioactive molecules, including nucleic acids, proteins, lipids and metabolites, can mediate specific cell-to-cell communication in the TME.[19] To better understand the factors in the TME that may trigger STING signaling in T cells, we collected exosomes from HeLa cells and the sera of healthy donors (C-EXOs) and applied them to Treg culture medium. We found that T-EXO treatment induced higher levels of STING, p-TBK1, p-IRF3 and FOXP3 than C-EXO treatment and Treg culture medium alone, although the C-EXOs induced a higher percentage of Treg differentiation than Treg culture medium alone (figure 6A,B). Furthermore, proteinase K-pretreated T-EXOs still induced higher levels of Tregs, STING, p-IRF3 and FOXP3 than the C-EXOs and Treg culture medium, suggesting that the nucleic acids carried by T-EXOs trigger STING signaling in T cells, leading to Treg induction (figure 6C,D). In addition, we also identified that T-EXOs from HeLa and SiHa cells enriched with TGF-β, a known factor that induces Treg induction, and the cGAS a known key molecule to STING pathway activation[6 20] (figure 6E). Importantly, we determined a high level of 2'-3'-cGAMP in T-EXOs by ELISA array (figure 6F). Moreover, we found that the promotion of T-EXO-induced iTreg differentiation was inhibited by TBK1-KD and IRF3-KD (online supplemental figure 6A,B). Meanwhile, the T-EXO from mouse TC-1 cells promoted iTreg differentiation from $CD4^+$-naïve T cells in WT mice but not TKO or $IRF3^{-/-}$ mice (figure 6G,H) and TC-1 exosome could activate IRF3 and TBK1 pathways (figure 6I). Additionally, we identified that TC-1 exosomes from TC-1 cells were enriched with TGF-β, cGAS, HPV16E6 and HPV16E7 (figure 6J). To further investigate the activation of STING in the TMEs of patients with CC, we isolated peripheral lymphocytes and fresh tumor-infiltrating lymphocytes (TILs) from patients with CC and observed a higher percentage of $CD4^+CD25^{high}FOXP3^+$ Tregs in fresh TILs than in peripheral lymphocytes and higher levels of FOXP3 and STING signaling pathway component proteins, including STING, p-TBK1 and p-IRF3, in the TILs (online supplemental figure 7A,B). Moreover, the transcript levels of STING, TGF-β, FOXP3, ISG20, ICOS, JUNB, PAK2, CD28 and BATF were higher in TILs than in peripheral lymphocytes as determined by qRT-PCR (online supplemental figure 7C).

DISCUSSION

Microbial infection, tumor DNA and self-damaging DNA are three vital factors that induce the activation of the cGAS-STING signaling pathway.[21] Boosting the cGAS-STING pathway in the cancer microenvironment reportedly promotes antitumor immunity, and multiple STING agonists have been developed for cancer therapy studies and shown promising preclinical results.[22–24] In the present study, the intratumoral STING level and $FOXP3^+$ cell infiltration was increased in HPV-positive patients with CC, and the intratumoral STING level was negatively associated with the $CD8^+$ cell density. Surprisingly, TC-1 tumor specimens from STING TKO mice showed decreased $FOXP3^+$ cell infiltration but increased $CD8^+$ cell infiltration relative to those of WT mice. These data suggest that activation of cGAS-STING signaling induces T cell-mediated immune tolerance in HPV-positive CC. We found that STING and $FOXP3^+$ cells were independent predictors of unfavorable outcomes for HPV-positive patients with CC and of a slower TC-1 tumor growth rate in TKO mice. These observations challenge the current prevailing assumption that STING signaling generally acts as a positive regulator of antitumor immunity.[25–27] It has been documented that the STING-knockout in $CD11b^+$ brain-infiltrating leukocytes leads to tumor progression

because of decreased I-IFN[28]; and intratumoral injection of STING agonists in murine model could inhibit tumor growth and increase infiltration of $CD8^+$ cytotoxic T cells.[29 30] Based on these contrasting roles of STING in antitumor immunity, we propose that the association between SITNG activation and immune tolerance in HPV-positive CC is due to the T cell-intrinsic function of STING.

Since the initial discovery of STING, myeloid cells have been the primary cell type of choice in most studies[31]; therefore, the role of STING in T cells is still obscure. STING activates many signaling pathways in T cells, the majority of which are IFN independent, and its role in T cells is distinct from antigen stimulation, T cell receptor (TCR) and costimulatory signals.[6] We here found that murine $CD4^+$ T cells with STING deficiency showed impaired iTreg differentiation induced by the TCR, interleukin-2 receptor (IL-2R) and TGF-β signaling in vitro despite the normal development of the lymphoid compartment in TKO mice relative to WT mice. Accordingly, we found that the empowerment of iTreg generation, including activation of the TCR, IL-2R signaling and TGF-β receptor (TGF-βR), could induce STING signaling activation in human and murine $CD4^+$ T cells. Consistently, we further revealed that ectopic STING expression altered the generation of iTregs from human $CD4^+$-naïve T cells in vitro. It is worth noting that STING agonists promoted iTreg generation from both murine and human $CD4^+$-naïve T cells. These data suggest that the activation of T cell-intrinsic STING cooperates with TCR, IL-2R and TGF-β signaling to modulate iTreg differentiation. Some studies revealed that activation of STING in T cells inhibits TCR-stimulated T cell proliferation and induces T cell apoptosis, which are independent of IFN-β signaling cascade to nuclear factor kappa B (NF-κB) activation.[31–34] Importantly, the researchers also pointed out that the STING-triggered cell apoptosis is cell-specific and dependent on the dose of the STING agonist.[32] In our in vitro experiments, we chose a low dose of STING agonist, including CMA and DMXAA (for mouse STING activation only), which could not induce the apoptosis of human and murine T cells (data not shown); furthermore, we did not observe a significant difference of iTreg proliferation under CM, high IL-2, TGF-β or STING agonist conditions in human and murine T cells with or without STING deficiency (online supplemental figure 3E-J).

Thus, the mechanism by which STING mediates iTreg generation requires further investigation. We found that the ability of $CD4^+$-naïve T cells from $IFNAR^{-/-}$ mice to generate iTreg differentiation was similar to that of the corresponding cells of WT mice in vitro, but the $CD4^+$ $IRF3^{-/-}$-naïve T cells showed a poor ability to induce Treg generation under the stimulation of the TCR and the cytokine IL-2 with or without TGF-β. For human T cells, ectopic TBK1 and IRF3 expression in human $CD4^+$ T cells altered iTreg generation, and deficiency of TBK1 or IRF3 reversed the STING-mediated and TGF-β-mediated iTreg promotion in vitro. Importantly, exogenous mouse or human IFN-β did not promote iTreg generation from $CD4^+$-naïve T cells in vitro. Our data indicate that TBK1 and IRF3, but not IFN-β, are required for the STING-mediated expansion of iTregs. Consistent with our results, early studies reported that activation of the STING/IFN-β pathway suppressed the effector and helper T-cell responses but activated FOXP3-lineage $CD4^+$ Tregs by inducing indoleamine 2,3-dioxygenase (IDO) to catabolize tryptophan.[35] Additionally, it has been reported that viral infection can trigger iTreg expansion in mice dependent on the type I IFN pathway.[36] Moreover, one recent study pointed out that exogenous INF-β could directly induce Treg from naïve $CD4^+$ T cells by STAT1-dependent and P300-dependent FOXP3 acetylation in a Treg cell-dependent murine transplant model.[37] Together, our results suggest that STING in T cells functions to induce iTreg generation through TBK1 and IRF3 but works independently of IFN-β. In addition, the type I IFN-independent activity of STING is usually linked to antiproliferation and cell death in T cells by activation of NF-κB signaling and autophagy, and it is reported that the C-terminal domain of STING activates NF-κB to inhibit T cell proliferation.[31 34] Here, we observed the increased p-IκBα and p-p65 levels in human and murine iTreg differentiation in the presence of STING agonist but not in T cells with STING deficiency (online supplemental figure 8A,B).

FOXP3 is a master regulator and a specific molecular marker for iTregs that differentiate from naïve T cells in the periphery and regulate the development of nTregs in the thymus.[38] Here, we found that activation of STING or TCR, IL-2R and TGF-β signaling could induce FOXP3 expression at the mRNA and protein levels in murine and human $CD4^+$ T cells, but murine $CD4^+$ T cells from TKO or $IRF3^{-/-}$ mice and human $CD4^+$ T cells with STING knockdown could not induce FOXP3 expression. However, STING activation did not enhance FOXP3 protein synthesis or decrease FOXP3 protein degradation (data not shown). Thus, we wondered whether STING induces the transcription of FOXP3, which is regulated by transcription factor complexes under the control of multiplex signaling pathways, including IL-2R, TGF-β and NF-κB.[39 40] Among these transcription factors, activated STAT5 induced by IL-2 and SMAD3 induced by TGF-β could bind to the FOXP3 gene locus, leading to the transactivation of FOXP3 expression.[40] In this study, we subsequently found that STING signaling activation promoted the phosphorylation of both Smad-3 and STAT5, and STAT5 blockade inhibited the promotion of iTreg generation and FOXP3 expression induced by STING agonists. Moreover, it is reported that NF-κB family member p65 and c-Rel are key transcription factors for enhanced FOXP3 expression in Treg by gp96.[41] Thus, our data suggest that $CD4^+$ T cell-intrinsic STING signaling and TCR and IL-2R signaling cooperate to regulate iTreg generation by upregulating STAT5/

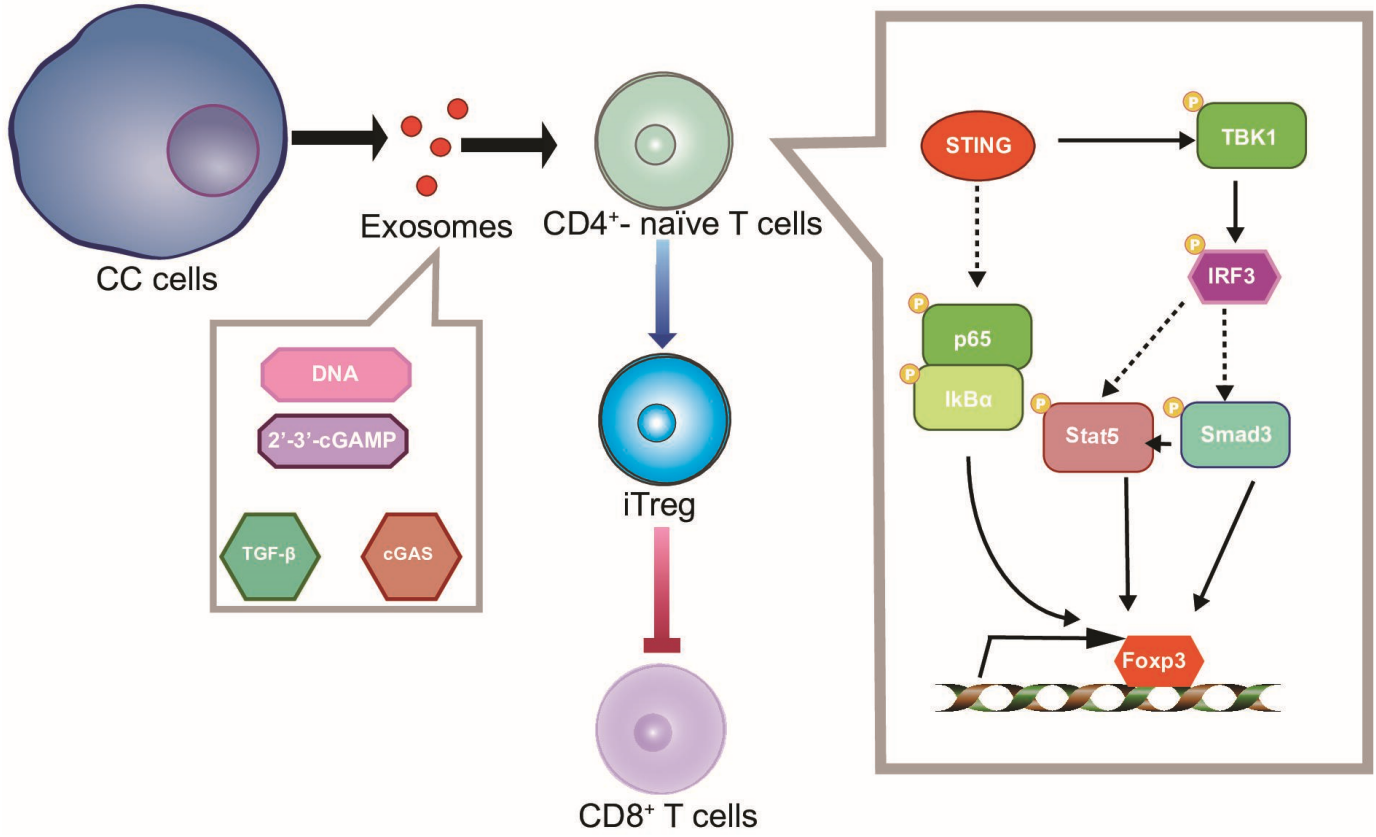

Figure 7 Cartoon schematic showing the regulatory mechanism of STING-mediated iTreg expansion in the CC tumor microenvironment. CC, cervical cancer; cGAS, cyclic GMP-AMP synthase; iTreg, regulatory T cell induction; STING, stimulator of interferon genes; TGF-β, transforming growth factor-beta.

SMAD3/NF-κB pathway-mediated FOXP3 transcription in vitro.

The mechanisms responsible for tumor-associated Treg expansion have been reported to be heterogeneous; here, we showed that STING signaling was activated in fresh TILs from patients with CC and $CD4^+$ T cells cocultured with CC cells in vitro. We hypothesize that STING-mediated Treg expansion is dependent on endogenous STING activation in tumor-infiltrated T cells. The acquisition of tumor DNA or tumor-derived cGAMP by immune cells has been reported to be the mechanism underlying extrinsic STING activation in the TME.[42–44] We further investigated additional factors that may induce T cell-intrinsic STING activation in the TME. Exosomes reportedly act as a bioinformatic messengers between tumor and immune cells.[45] Some researchers found that T-EXOs from irradiated breast cancer cells could activate STING signaling in dendritic cells to stimulate stronger antitumor immunity.[46] T-EXOs isolated from Epstein-Barr virus-positive nasopharyngeal carcinoma cells have been shown to induce Treg expansion.[47] Thus, we assessed whether T-EXOs from CC cells could induce STING activation in tumor-infiltrated T cells and found that T-EXOs from CC-derived cells as well as T-EXOs carrying DNA-induced iTreg differentiation and STING signal activation in vitro. Additionally, we found that cGAS, a key factor of STING signals, and TGF-β, a recognized cytokine promoting iTreg generation, was enriched in T-EXOs from CC cells.[20 40] An early study reported that in human HPV infection-associated oral cancer, activated STING promoted Treg infiltration via the c-jun/CCL22 signal, resulting in tumorigenesis.[48] The role of STING in tumor growth is still controversial; activating the STING pathway reportedly results in the release of its downstream inflammatory cytokines, including tumor necrosis factor-α, while chronic inflammatory factors have tumor-infiltrating effects, thereby promoting tumorigenesis.[49 50] STING activation has also been shown to directly promote tumor growth by inducing IDO activity in cancers with low antigenicity, such as murine Lewis lung carcinoma.[51] STING deficiency in mice has been shown to have antagonistic effects on 7,12-dimethylbenz[a]anthracene-induced skin cancer.[52] Inhibitors targeting STING may be important for the treatment of neurodegenerative and autoimmune diseases.[53 54] Recently, some researchers pointed out that small-molecule STING inhibitors such as aspirin and Astin-C have great potential for improving the treatment of human cancers.[55 56] Moreover, our data on the regulatory effects of STING signaling on tumor-associated Treg expansion provide a theoretical basis for the development of immunotherapy strategies targeting STING inhibition in HPV-positive CCs in the near future.

In summary, we here found that T cell-intrinsic STING signaling is activated by T-EXOs, which carry

tumor-derived or HPV-derived DNA and proteins, such as TGF-β, from tumor cells and then cooperate with other T cell signals, including TCR, IL-2R and TGF-β signals, to promote iTreg expansion, resulting in immune suppression and poor outcomes in CC (figure 7).

Author affiliations
[1]State Key Laboratory of Oncology in South China, Collaborative Innovation Center for Cancer Medicine, Sun Yat-sen University Cancer Center, Guangzhou, People's Republic of China
[2]Department of Biotherapy, Sun Yat-sen University Cancer Center, Guangzhou, People's Republic of China
[3]Department of Gynecological Oncology, Sun Yat-sen University Cancer Center, Guangzhou, People's Republic of China
[4]Department of Experiment Medicine, Sun Yat-sen University Cancer Center, Guangzhou, People's Republic of China

Contributors JL and XX conceived and designed the study. HN and HZ conducted most experiments and wrote the manuscript. LL performed some key experiments. HH, HG, LZ, CL, J-XX, C-PN and KL performed parts of the involved experiments. XZ provided reagents and analyzed data. JL and XX supervised the project and revised the manuscript. JL is the guarantor of this study.

Funding This work was supported by the National Natural Science Foundation of China (grant nos. 81972874, 81773256, 81572982, 81773051, 81972692 and 81902905), the Sci Tech Key Program of the Guangzhou City Science Foundation (grant no. 201802020001), the Guangdong Province Sci-Tech International Key Program (grant no. 2021A0505030027) and the Guangdong Innovative and Entrepreneurial Research Team Program (grant no. 2016ZT06S638).

Competing interests The authors declare no competing interests.

Patient consent for publication Not applicable.

Ethics approval This study was approved by Research Ethics Committee of Sun Yat-sen University Cancer Center (CZR2019-238). Participants gave informed consent to participate in the study before taking part. The data authenticity of this article has been validated by uploading the key raw data onto the Research Data Deposit platform (www.researchdata.org.cn) and inspected/approved by the Sun Yat-sen University Cancer Center Data Access/Ethics Committee with the approval number RDDB2022519092.

Provenance and peer review Not commissioned; externally peer reviewed.

Data availability statement Data are available on reasonable request.

ORCID iD
Xiaojun Xia http://orcid.org/0000-0003-4444-7472

REFERENCES

1 Lv M, Chen M, Zhang R, *et al*. Manganese is critical for antitumor immune responses via cGAS-STING and improves the efficacy of clinical immunotherapy. *Cell Res* 2020;30:966–79.
2 Marcus A, Mao AJ, Lensink-Vasan M, *et al*. Tumor-Derived cGAMP triggers a STING-mediated interferon response in non-tumor cells to activate the NK cell response. *Immunity* 2018;49:754–63.
3 Woo S-R, Corrales L, Gajewski TF. Innate immune recognition of cancer. *Annu Rev Immunol* 2015;33:445–74.
4 Iurescia S, Fioretti D, Rinaldi M. Nucleic acid sensing machinery: targeting innate immune system for cancer therapy. *Recent Pat Anticancer Drug Discov* 2018;13:2–17.
5 Wu J-J, Zhao L, Hu H-G, *et al*. Agonists and inhibitors of the STING pathway: potential agents for immunotherapy. *Med Res Rev* 2020;40:1117–41.
6 Imanishi T, Saito T. T cell co-stimulation and functional modulation by innate signals. *Trends Immunol* 2020;41:200–12.
7 Domvri K, Petanidis S, Zarogoulidis P, *et al*. Treg-dependent immunosuppression triggers effector T cell dysfunction via the STING/ILC2 axis. *Clin Immunol* 2021;222:108620.
8 Field CS, Baixauli F, Kyle RL, *et al*. Mitochondrial integrity regulated by lipid metabolism is a cell-intrinsic checkpoint for Treg suppressive function. *Cell Metab* 2020;31:422–37.
9 Berman TA, Schiller JT. Human papillomavirus in cervical cancer and oropharyngeal cancer: one cause, two diseases. *Cancer* 2017;123:2219–29.
10 Polman NJ, Snijders PJF, Kenter GG, *et al*. HPV-based cervical screening: rationale, expectations and future perspectives of the new Dutch screening programme. *Prev Med* 2019;119:108–17.
11 Lo Cigno I, Calati F, Albertini S, *et al*. Subversion of host innate immunity by human papillomavirus oncoproteins. *Pathogens* 2020;9. doi:10.3390/pathogens9040292. [Epub ahead of print: 17 04 2020].
12 Saulters E, Woolley JF, Varadarajan S, *et al*. Stinging viral tumors: what we know from head and neck cancers. *Cancer Res* 2021;81:3945–52.
13 Bortnik V, Wu M, Julcher B, *et al*. Loss of HPV type 16 E7 restores cGAS-STING responses in human papilloma virus-positive oropharyngeal squamous cell carcinomas cells. *J Microbiol Immunol Infect* 2021;54:733-739.
14 Yogev O, Henderson S, Hayes MJ, *et al*. Herpesviruses shape tumour microenvironment through exosomal transfer of viral microRNAs. *PLoS Pathog* 2017;13:e1006524.
15 Marzagalli M, Ebelt ND, Manuel ER. Unraveling the crosstalk between melanoma and immune cells in the tumor microenvironment. *Semin Cancer Biol* 2019;59:236–50.
16 Kato K, Omura H, Ishitani R, *et al*. Cyclic GMP-AMP as an endogenous second messenger in innate immune signaling by cytosolic DNA. *Annu Rev Biochem* 2017;86:541–66.
17 Bao R, Hou J, Li Y, *et al*. Adenosine promotes FOXP3 expression in Treg cells in sepsis model by activating JNK/AP-1 pathway. *Am J Transl Res* 2016;8:2284–92.
18 Ruan Q, Kameswaran V, Tone Y, *et al*. Development of FOXP3(+) regulatory t cells is driven by the c-Rel enhanceosome. *Immunity* 2009;31:932–40.
19 Mashouri L, Yousefi H, Aref AR, *et al*. Exosomes: composition, biogenesis, and mechanisms in cancer metastasis and drug resistance. *Mol Cancer* 2019;18:75.
20 Hopfner K-P, Hornung V. Molecular mechanisms and cellular functions of cGAS-STING signalling. *Nat Rev Mol Cell Biol* 2020;21:501–21.
21 Yang Q, Shu H-B. Deciphering the pathways to antiviral innate immunity and inflammation. *Adv Immunol* 2020;145:1–36.
22 Mullins SR, Vasilakos JP, Deschler K, *et al*. Intratumoral immunotherapy with TLR7/8 agonist MEDI9197 modulates the tumor microenvironment leading to enhanced activity when combined with other immunotherapies. *J Immunother Cancer* 2019;7:244.
23 Schadt L, Sparano C, Schweiger NA, *et al*. Cancer-Cell-Intrinsic cGAS expression mediates tumor immunogenicity. *Cell Rep* 2019;29:1236–48.
24 Zhou Y, Fei M, Zhang G, *et al*. Blockade of the phagocytic receptor MERTK on tumor-associated macrophages enhances P2X7R-Dependent sting activation by tumor-derived cGAMP. *Immunity* 2020;52:357–73.
25 Ohkuri T, Kosaka A, Ishibashi K, *et al*. Intratumoral administration of cGAMP transiently accumulates potent macrophages for anti-tumor immunity at a mouse tumor site. *Cancer Immunology, Immunotherapy* 2017;66:705–16.
26 Takahashi M, Lio C-WJ, Campeau A, *et al*. The tumor suppressor kinase DAPK3 drives tumor-intrinsic immunity through the STING-IFN-β pathway. *Nat Immunol* 2021;22:485–96.
27 Takashima K, Oshiumi H, Matsumoto M, *et al*. TICAM-1 is dispensable in STING-mediated innate immune responses in myeloid immune cells. *Biochem Biophys Res Commun* 2018;499:985–91.
28 Ohkuri T, Ghosh A, Kosaka A, *et al*. STING contributes to antiglioma immunity via triggering type I IFN signals in the tumor microenvironment. *Cancer Immunol Res* 2014;2:1199–208.

29 Jing W, McAllister D, Vonderhaar EP, *et al*. STING agonist inflames the pancreatic cancer immune microenvironment and reduces tumor burden in mouse models. *J Immunother Cancer* 2019;7:115.
30 Shi F, Su J, Wang J, *et al*. Activation of STING inhibits cervical cancer tumor growth through enhancing the anti-tumor immune response. *Mol Cell Biochem* 2021;476:1015–24.
31 Wu J, Dobbs N, Yang K, *et al*. Interferon-Independent activities of mammalian sting mediate antiviral response and tumor immune evasion. *Immunity* 2020;53:115–26.
32 Gulen MF, Koch U, Haag SM, *et al*. Signalling strength determines proapoptotic functions of STING. *Nat Commun* 2017;8:427.
33 Larkin B, Ilyukha V, Sorokin M, *et al*. Cutting edge: activation of sting in T cells induces type I IFN responses and cell death. *J Immunol* 2017;199:397–402.
34 Cerboni S, Jeremiah N, Gentili M, *et al*. Intrinsic antiproliferative activity of the innate sensor STING in T lymphocytes. *J Exp Med* 2017;214:1769–85.
35 Lemos H, Huang L, McGaha TL, *et al*. Cytosolic DNA sensing via the stimulator of interferon genes adaptor: Yin and Yang of immune responses to DNA. *Eur J Immunol* 2014;44:2847–53.
36 Ager CR, Reilley MJ, Nicholas C, *et al*. Intratumoral sting activation with T-cell checkpoint modulation generates systemic antitumor immunity. *Cancer Immunol Res* 2017;5:676–84.
37 Fueyo-González F, McGinty M, Ningoo M, *et al*. Interferon-β acts directly on T cells to prolong allograft survival by enhancing regulatory T cell induction through Foxp3 acetylation. *Immunity* 2022;55:459–74.
38 Li C, Jiang P, Wei S, *et al*. Regulatory T cells in tumor microenvironment: new mechanisms, potential therapeutic strategies and future prospects. *Mol Cancer* 2020;19:116.
39 Copland A, Bending D. FOXP3 molecular dynamics in Treg in juvenile idiopathic arthritis. *Front Immunol* 2018;9:2273.
40 Wing JB, Tanaka A, Sakaguchi S. Human FOXP3^{+} Regulatory T Cell Heterogeneity and Function in Autoimmunity and Cancer. *Immunity* 2019;50:302–16.
41 Xu Y, Liu E, Xie X, *et al*. Induction of FOXP3 and activation of Tregs by HSP gp96 for treatment of autoimmune diseases. *iScience* 2021;24:103445.
42 Corrales L, Matson V, Flood B, *et al*. Innate immune signaling and regulation in cancer immunotherapy. *Cell Res* 2017;27:96–108.
43 Demaria O, De Gassart A, Coso S, *et al*. STING activation of tumor endothelial cells initiates spontaneous and therapeutic antitumor immunity. *Proc Natl Acad Sci U S A* 2015;112:15408–13.
44 Woo S-R, Fuertes MB, Corrales L, *et al*. STING-dependent cytosolic DNA sensing mediates innate immune recognition of immunogenic tumors. *Immunity* 2014;41:830–42.
45 Daassi D, Mahoney KM, Freeman GJ. The importance of exosomal PDL1 in tumour immune evasion. *Nat Rev Immunol* 2020;20:209–15.
46 Taghikhani A, Hassan ZM, Ebrahimi M, *et al*. microRNA modified tumor-derived exosomes as novel tools for maturation of dendritic cells. *J Cell Physiol* 2019;234:9417–27.
47 Mrizak D, Martin N, Barjon C, *et al*. Effect of nasopharyngeal carcinoma-derived exosomes on human regulatory T cells. *J Natl Cancer Inst* 2015;107:363.
48 Liang D, Xiao-Feng H, Guan-Jun D, *et al*. Activated STING enhances Tregs infiltration in the HPV-related carcinogenesis of tongue squamous cells via the c-jun/CCL22 signal. *Biochim Biophys Acta* 2015;1852:2494–503.
49 Liu K, Lan Y, Li X, *et al*. Development of small molecule inhibitors/agonists targeting STING for disease. *Biomed Pharmacother* 2020;132:110945.
50 Khoo LT, Chen L-Y. Role of the cGAS-STING pathway in cancer development and oncotherapeutic approaches. *EMBO Rep* 2018;19. doi:10.15252/embr.201846935. [Epub ahead of print: 16 11 2018].
51 Lemos H, Mohamed E, Huang L, *et al*. STING promotes the growth of tumors characterized by low antigenicity via IDO activation. *Cancer Res* 2016;76:2076–81.
52 Ahn J, Xia T, Konno H, *et al*. Inflammation-driven carcinogenesis is mediated through sting. *Nat Commun* 2014;5:5166.
53 Haag SM, Gulen MF, Reymond L, *et al*. Targeting STING with covalent small-molecule inhibitors. *Nature* 2018;559:269–73.
54 Deng Z, Chong Z, Law CS, *et al*. A defect in COPI-mediated transport of STING causes immune dysregulation in COPA syndrome. *J Exp Med* 2020;217. doi:10.1084/jem.20201045. [Epub ahead of print: 02 11 2020].
55 Zhu X, Han W, Liu Y, *et al*. Rational design of a prodrug to inhibit self-inflammation for cancer treatment. *Nanoscale* 2021;13:5817–25.
56 Li S, Hong Z, Wang Z, *et al*. The cyclopeptide Astin C specifically inhibits the innate immune CDN sensor sting. *Cell Rep* 2018;25:3405–21.